Laser and Particle Beams (2009), *27*, 579–585.

doi:10.1017/S0263034609990292

Laser pulse compression and amplification via Raman backscattering in plasma

ASHUTOSH SHARMA AND IOANNIS KOURAKIS

Centre for Plasma Physics, School of Mathematics and Physics, Queen's University, Belfast, Northern Ireland, United Kingdom

(RECEIVED 23 January 2009; ACCEPTED 4 July 2009)

Abstract

A simple theoretical model is proposed for the interaction between two counter-propagating laser pulses (a pump and a seed pulse) in unmagnetized plasma. Pulse compression and amplification are observed *via* numerical simulation. A one dimensional fluid model for stimulated Raman backscattering is proposed to investigate the pulse compression and pulse amplification mechanisms. To accomplish this, energy is transferred from the long pump pulse to a seed pulse, with a Langmuir plasma wave mediating the transfer. The study focuses on the intensity profile of the pump laser pulse. A Gaussian and a ring intensity profile are, separately, considered for the pump laser pulse.

Keywords: Compression; Pulse amplification; Raman backscattering

1. INTRODUCTION

The generation of ultraintense subpicosecond and femtosecond laser pulses is crucial for a number of scientific and technical applications, such as plasma-based particle accelerators (Tajima, 1985; Giulietti *et al.*, 2005; Joshi, 2006), inertial confinement fusion (ICF) (Borisenko *et al.*, 2008; Deutsch *et al.*, 2008; Eliezer *et al.*, 2007; Hora, 2007*a*, 2007*b*; Kline *et al.*, 2009; Rodriguez *et al.*, 2008; Romagnani *et al.*, 2008; Seifter *et al.*, 2009; Winterberg, 2008; Zvorykin *et al.*, 2007), and X-ray lasers (Eder *et al.*, 1992; Faenov *et al.*, 2007). For example, with the help of lasers whose intensity at the lens focus is about 10^{23} W/cm^2, one can investigate nuclear reactions (Renner *et al.*, 2008) and the effects of nonlinear quantum electrodynamics (Andreev, 2002). The standard method for obtaining ultrashort laser pulses is a compression of an electromagnetic (EM) pulse with given energy *via* chirped-pulse amplification (CPA) scheme (Strickland & Mourou, 1985; Kalashnikov *et al.*, 2007). In this scheme, a laser beam is amplified and then compressed using dispersion effects of linear optics. CPA based optical systems have been shown to generate subpicosecond petawatt laser pulses (Mourou *et al.*, 1998; Key *et al.,* 1998) with up to 500 J per pulse. The pulse energy is limited by the thermal damage to the compression gratings, which become large and expensive for KJ pulses. A possible route to increase peak intensity is to decrease pulse duration, which can be achieved by using broad bandwidth parametric amplifiers (Ross *et al.*, 1997). This does not however ease the energy restriction.

Another method for obtaining ultraintense laser pulses, which was proposed by Maier *et al.* (1966), is nonlinear compression based on stimulated scattering processes, which requires no preliminary time broadening of laser pulses. Approximately 70% of the energy of a high-power laser pulse of long duration can be transformed into a shorter signal (30-fold shorter under optimal conditions) by focusing of the initial pulse into a nonlinear medium (Andreev *et al.*, 2007). It was shown experimentally that, in a nonlinear gaseous medium, a short seed pulse ($t_s < 1$ ns) can be significantly amplified in the course of its interaction with a counter-propagating pump wave of a longer duration (with an energy of about 1 KJ and duration $t_l > 20$ ns) (Gorbunov *et al.*, 1983). The superradiant amplification (Shvets *et al.*, 1998) of an ultrashort laser pulse by a counter-propagating long low-intensity pump has been explored. The superradiant amplification occurs if the frequency of the pulse is lower than that of the pump, and the initial pulse intensity is sufficiently high. Recent investigation (Ren *et al.*, 2007) for generating ultraintense and ultrashort laser pulses, report the use of stimulated Raman backscattering in millimetre-scale plasma to simultaneously amplify and compress an input

Address correspondence and reprint requests to: Ashutosh Sharma, Centre for Plasma Physics, School of Mathematics and Physics, Queen's University, Belfast, Northern Ireland, United Kingdom. E-mail: a.sharma@qub.ac.uk or a_physics2001@yahoo.com

pulse to increase its intensity by more than two orders of magnitude. Further amplification and compression of such a pulse was achieved by passing it twice through the system.

In this article, we study a scheme for generating compressed femtosecond laser pulses with a repetition rate either the same as or greatly enhanced from that of the pump pulse. We also focus our study on the intensity profile of pump laser pulse. The Gaussian and ring intensity profile have been considered to amplify the seed laser pulse. In our model, we have considered the Raman backscattering (RBS) process. This approach relies on pulse interaction with a plasma medium used to amplify the ultraintense laser pulse. To accomplish this, energy is transferred from a long pump laser pulse at frequency ω_0 to an intense seed pulse at frequency ω_s, with an electron plasma wave at frequency ω_p mediating the transfer. The frequencies are chosen to satisfy the resonant condition

$$\omega_p = \omega_0 - \omega_s.$$

This model of RBS involves the interaction of (1) an incident long laser pulse (EM wave), the so called pump, (2) a short seed laser pulse (EM wave), the so called pumped wave, (3) an electron plasma wave (electrostatic field). RBS involves two types of waves: a transverse EM wave, and an electron plasma wave (EPW). Using the fluid model, we have derived the wave equations corresponding to the transverse EM wave and electron EPW. One further assumes the system to be one-dimensional, so that all fields depend on a single spatial variable x.

2. MATHEMATICAL MODEL

The two coupled equations for the transverse EM wave with vector potential component A_z and EPW with electrostatic component E_x read:

$$\frac{\partial^2 A_z}{\partial t^2} - c^2\frac{\partial^2 A_z}{\partial x^2} + \omega_p^2 A_z = \frac{e}{m}\frac{\partial E_x}{\partial x}A_z, \tag{1}$$

$$\frac{\partial^2 E_x}{\partial t^2} - 3v_{th}^2\frac{\partial^2 E_x}{\partial x^2} + \omega_p^2 E_x = -\omega_p^2\frac{1}{2}\frac{\partial}{\partial x}\left(\frac{eA_z^2}{m}\right), \tag{2}$$

where $\omega_p^2 = N_0\, e^2/\in_0 m$ is the plasma frequency and N_0 is the unperturbed electron density.

The vector potential field A_z in Eq. (1) is the superposition of the pump laser field propagating in the positive x direction and the seed laser pulse in the negative x-direction. The left-hand-side of the Eq. (1) is simply the linear wave equation for transverse EM waves, giving rise to the dispersion relation $\omega_0^2 = \omega_p^2 + c^2 k_0^2$, and in particular to the well known condition for propagation $|\omega| > \omega_p$. E_x on the right-hand-side of Eq. (1) and in Eq. (2) is the Langmuir wave electrostatic field related to the electron plasma waves. Since the longitudinal electron plasma waves are naturally a source of density fluctuations, the term on the right-hand-side of Eq. (1) accounts for nonlinear coupling between the transverse EM waves and the plasma waves.

The vector potential field A_z can be written as

$$\begin{aligned} A_z(x,t) = &\frac{1}{2}[A_0(x,t)\, exp\, i(k_0 x - \omega_0 t) + c.c.] \\ &+ \frac{1}{2}[A_s(x,t)\, exp\, i(k_s x - \omega_s t) + c.c.], \end{aligned} \tag{3}$$

while a similar ansatz is considered for the electrostatic field:

$$E_x(x,t) = \frac{1}{2}[E(x,t)\, exp\, i(k_e x - \omega_e t) + c.c.], \tag{4}$$

where the wave number—frequency pairs (k, ω) of all three waves verify their respective linear dispersion relations:

$$\omega_0^2 = \omega_p^2 + c^2 k_0^2, \tag{5a}$$

$$\omega_s^2 = \omega_p^2 + c^2 k_s^2, \tag{5b}$$

$$\omega_e^2 = \omega_p^2 + 3v_{th}^2 k_e^2; \tag{5c}$$

where ω_0, ω_s and ω_e are the pump laser, seed laser and electron plasma frequencies and k_0, k_s and k_e are the corresponding wave numbers.

To obtain the evolution equations for the amplitudes A_0 and A_s for the pump and seed laser pulses, we substitute the expression for A_z and E_x from Eqs. (3) and (4) in Eq. (1). The substitution leads to:

$$\begin{aligned} &\frac{1}{2}\left[\left(\frac{\partial^2 A_0}{\partial t^2} - 2i\omega_0\frac{\partial A_0}{\partial t}\right) exp\, i(k_0 x - \omega_0 t) + c.c.\right] \\ &- c^2\frac{1}{2}\left[\left(\frac{\partial^2 A_0}{\partial x^2} + 2ik_0\frac{\partial A_0}{\partial x}\right) exp\, i(k_0 x - \omega_0 t) + c.c.\right] \\ &+ \frac{1}{2}\left[\left(\frac{\partial^2 A_s}{\partial t^2} - 2i\omega_s\frac{\partial A_s}{\partial t}\right) exp\, i(k_s x - \omega_s t) + c.c.\right] \\ &- c^2\frac{1}{2}\left[\left(\frac{\partial^2 A_s}{\partial x^2} + 2ik_s\frac{\partial A_s}{\partial x}\right) exp\, i(k_s x - \omega_s t) + c.c.\right] \\ &= \frac{e}{m}\frac{1}{2}\left[\left(\frac{\partial E}{\partial x} + ik_e E\right) exp\, i(k_e x - \omega_e t) + c.c.\right] \\ &\times \left\{\frac{1}{2}[A_0\, exp\, i(k_0 x - \omega_0 t) + c.c.]\right. \\ &\left. + \frac{1}{2}[A_s\, exp\, i(k_s x - \omega_s t) + c.c.]\right\}, \end{aligned} \tag{6}$$

having made use of Eqs. (5a, 5b). By multiplying Eq. (6) by exp[-$i(k_0 x - \omega_0 t)$] and then averaging Eq. (6) over the fast time scales (i.e., for evolution time longer than the reciprocal of electron plasma frequency) and fast spatial scale, one obtains an equation for the pump laser pulse amplitude A_0 (x,t) evolving on a slow variation scale $\left(\left|\frac{1}{A_0}\frac{\partial A_0}{\partial x}\right| << |k_0| \text{ and } \left|\frac{1}{A_0}\frac{\partial A_0}{\partial t}\right| << |\omega_0|\right)$. We observe that the nonlinear coupling terms on the

https://doi.org/10.1017/S0263034609990292 Published online by Cambridge University Press

right-hand-side of Eq. (6) will in general average out to zero unless certain resonant conditions are met. These conditions correspond to phase matching of the three waves both is space and time, and can be written in terms of the wave numbers and frequencies as:

$$k_0 = k_s + k_e, \tag{7a}$$

$$\omega_0 = \omega_s + \omega_e + \delta\omega. \tag{7b}$$

Having allowed in Eq. (7b) for a possible frequency mismatch $\delta\omega$, such that $|\delta\omega| \ll |\omega_{0,s,e}|$. Under these matching conditions, we obtain after averaging:

$$\frac{\partial A_0}{\partial t} + \frac{i}{2}\frac{1}{\omega_0}\frac{\partial^2 A_0}{\partial t^2} + c^2\frac{k_0}{\omega_0}\frac{\partial A_0}{\partial x} = -\frac{e}{4m}\frac{k_e}{\omega_0} E A_s \exp(i\delta\omega t). \tag{8}$$

Similarly, multiplying Eq. (6) by $\exp[-i(k_s x - \omega_s t)]$ and performing the same averaging leads to the corresponding equation for the seed pulse amplitude $A_s(x, t)$:

$$\frac{\partial A_s}{\partial t} + \frac{i}{2}\frac{1}{\omega_s}\frac{\partial^2 A_s}{\partial t^2} + c^2\frac{k_s}{\omega_s}\frac{\partial A_s}{\partial x} = \frac{e}{4m}\frac{k_e}{\omega_s} E^* A_0 \exp(-i\delta\omega t). \tag{9}$$

The equation for the EPW envelope $E(x, t)$ is obtained through a similar derivation by inserting Eq. (3) and Eq. (4) into Eq. (2), multiplying by $\exp[-i(k_e x - \omega_e t)]$, and averaging. Using the phase matching conditions, we obtain,

$$\frac{\partial E}{\partial t} + \frac{i}{2}\frac{1}{\omega_e}\frac{\partial^2 E}{\partial t^2} + 3v_{th}^2\frac{k_e}{\omega_e}\frac{\partial E}{\partial x} = \frac{e}{4m}\frac{k_e}{\omega_e}\omega_p^2 A_0 A_s^* \exp(-i\delta\omega t). \tag{10}$$

Transforming Eqs. (8–10) for the pump laser field, seed field and electron plasma wave field into the dimensionless form, we obtain:

$$\frac{\partial a_0}{\partial \xi} + \frac{i}{2}\frac{\omega_p}{ck_0}\frac{\partial^2 a_0}{\partial \tau^2} = -\frac{k_e}{4}\frac{c^2}{\omega_0 v_{g,0}}\varepsilon\, a_s \exp(i\delta\omega t), \tag{11}$$

$$\frac{\partial a_s}{\partial \xi} + \frac{i}{2}\frac{\omega_p}{ck_s}\frac{\partial^2 a_s}{\partial \tau^2} + c\left(\frac{1}{v_{g,s}} - \frac{1}{v_{g,0}}\right)\frac{\partial a_s}{\partial \tau} = \frac{k_e}{4}\frac{c^2}{\omega_s v_{g,s}} a_0\, \varepsilon^* \exp(-i\delta\omega t), \tag{12}$$

$$\frac{\partial \varepsilon}{\partial \xi} + \frac{i}{2}\frac{\omega_p c}{3v_{th}^2 k_e}\frac{\partial^2 \varepsilon}{\partial \tau^2} + c\left(\frac{1}{v_{g,e}} - \frac{1}{v_{g,0}}\right)\frac{\partial \varepsilon}{\partial \tau} = \frac{k_e}{4}\frac{c^2}{\omega_e}\frac{1}{v_{g,e}} a_0\, a_s^* \exp(-i\delta\omega t), \tag{13}$$

where

$$a_{0,s} = \frac{eA_{0,s}}{mc^2},\ \varepsilon = \frac{eE}{mc\omega_p},\ v_{g,0} = \frac{c^2 k_0}{\omega_0},\ v_{g,s} = \frac{c^2 k_s}{\omega_s},$$

$$\xi = \frac{\omega_p}{c}x \text{ and } \tau = \left(t - \frac{x}{v_{g,0}}\right)\omega_p.$$

3. NUMERICAL RESULTS AND DISCUSSION

We have carried out a numerical simulation of the seed pulse amplification in the Raman backscattering regime by solving the three coupled equations (Eqs. (11)–(13)) for the pump, seed, and plasma wave fields. The amplification of the seed pulse is demonstrated as it propagates through 4 cm of plasma while interacting with a counter-propagating pump pulse (pulse length = 20 ps) whose frequency is 3% higher. The plasma has a uniform density of $n_0 = 1.0 \times 10^{19}\ \mathrm{cm}^{-3}$ and Rayleigh length = 50 μm. The seed and the plasma wavelengths were set to meet the matching condition given by Eq. (7a). The numerical simulation is performed for two cases corresponding to different pump field distributions. In the first case, we have considered the pump field distribution to obey a Gaussian longitudinal profile, while in the second case, the field distribution for the pump is described by a ring shaped longitudinal profile. The numerical simulation is performed by using a one-dimensional solver, PDEPE, supplied by MATLAB (The Math Works). The solver has an adequate set of methods for noncritical initial–boundary value problems for systems of parabolic and elliptical partial differential equations in one space variable and time.

Case 1: We have numerically investigated the amplification of a seed laser pulse by considering a long Gaussian pump with duration of 20 ps. The initial full width at half maximum is 1.18 times the pulse duration. The dimensionless vector potential of the laser defined as $a_0 = eA_0/\mathrm{mc}^2$, is 0.048 for the pump which corresponds to a laser intensity of 4.5 $\mathrm{PW/cm}^2$. The initial pump amplitude can be adjusted by changing the laser intensity or spot sizes in the experiments. The wavelength of the pump was set to be 0.832 μm. The dimensionless vector potential ($a_s = eA_s/\mathrm{mc}^2$) of the seed laser was chosen to be 1.6×10^{-4}. The initial seed pulse has duration of 20 ps. The intensity distribution of the seed pulse is initially considered to be a Gaussian one.

In our simulation, the amplification of a seed pulse was observed as it interacts with a counter-propagating long Gaussian pump pulse inside the plasma. The maxima of the initial seed laser intensity coincide with the pump peak in the temporal domain. The results of this simulation are shown in Figures 1 and 2. Figure 1a shows a depletion of the long pump laser pulse at about 2 cm of plasma length and a depletion of the sidebands of the pump pulse further at the end of the plasma. Figure 1b shows an increase in intensity of the seed pulse counter-propagating through the pump. Energy is transferred from the left propagating long pump pulse to the right propagating short seed pulse (here left/right denotes the direction toward negative/positive values of x) with a Langmuir plasma wave at frequency ω_p mediating the transfer. Figure 1c shows the growth of the plasma wave field as a consequence of coupled pump laser field and seed pulse field. The initial intensity distribution of the Gaussian seed pulse is shown in Figure 2a.

https://doi.org/10.1017/S0263034609990292 Published online by Cambridge University Press

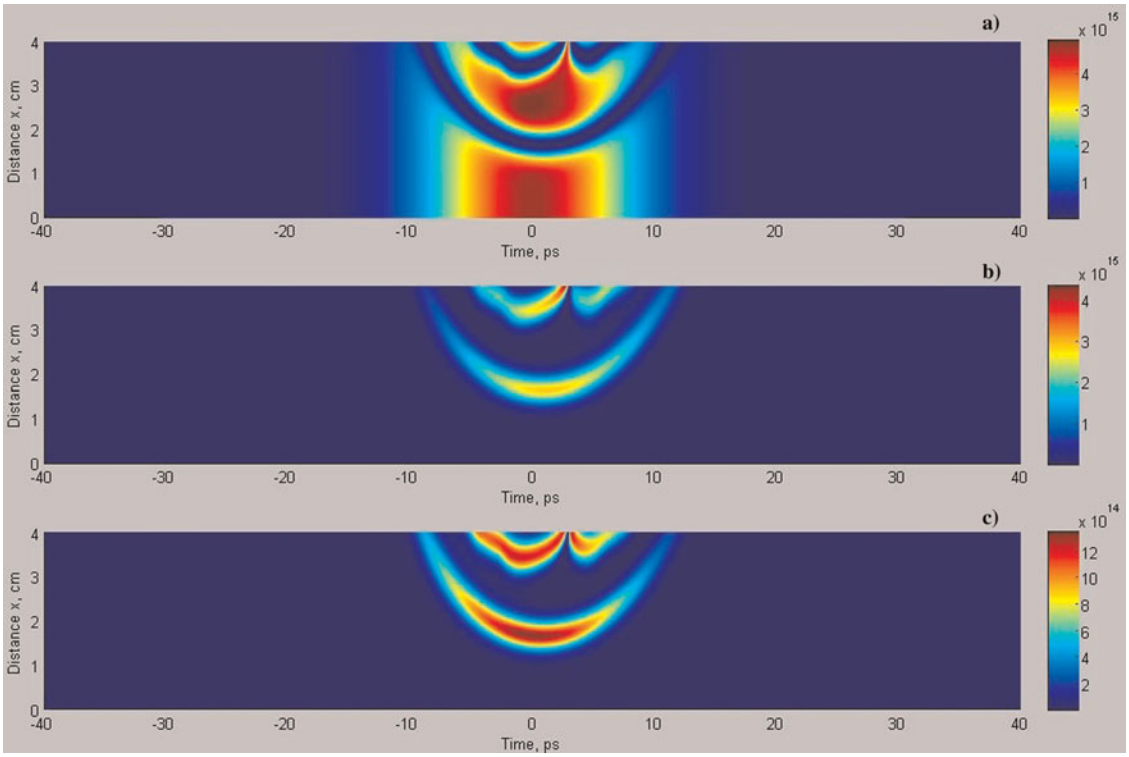

Fig. 1. (Color online) (**a**) The intensity distribution of the pump pulse, (**b**) the intensity distribution of the seed pulse, and (**c**) the intensity distribution of the plasma wave field are depicted for pump having Gaussian intensity distribution. The *x* axis represents the time scale compared to the travelling coordinate of the pump; the *y* axis represents the propagation distance. The red colour corresponds to the highest intensity, and the blue colour corresponds to near-zero intensity.

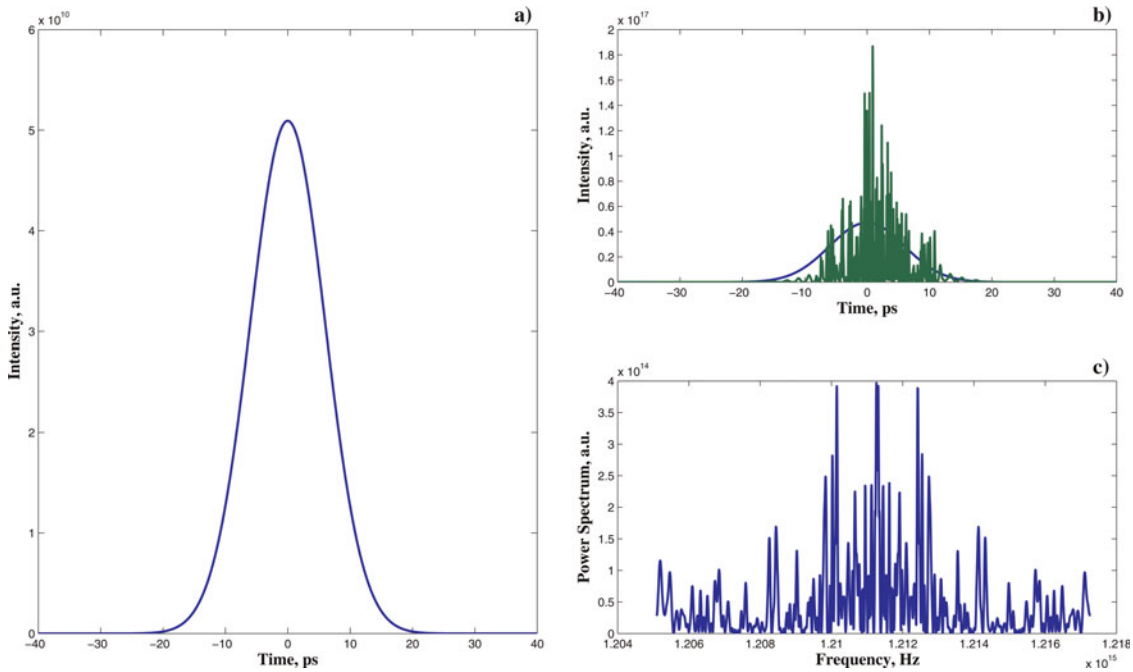

Fig. 2. (Color online) (**a**) The initial intensity profile of the Gaussian seed pulse, (**b**) the intensity profile of the amplified seed pulse (bell-shaped green erratic curve) is depicted in comparison with the intensity profile of the initial pump (the blue curve), and (**c**) the power spectrum of the amplified seed pulse for an initially Gaussian pump pulse.

https://doi.org/10.1017/S0263034609990292 Published online by Cambridge University Press

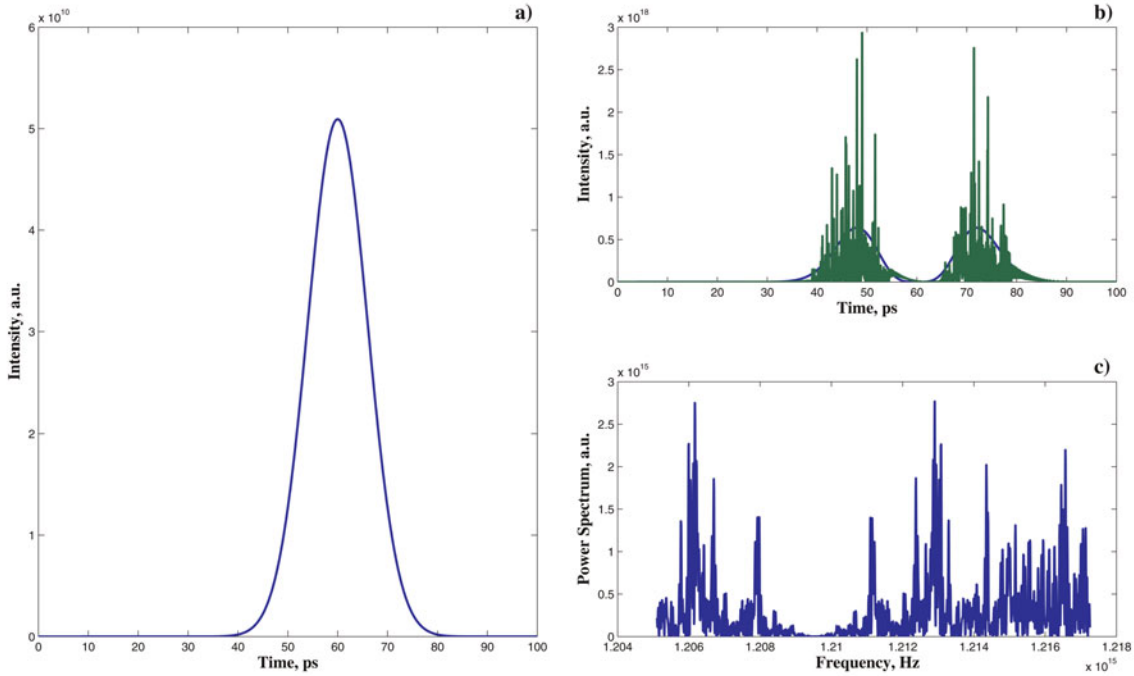

Fig. 3. (Color online) (**a**) The initial intensity profile of the Gaussian seed pulse, (**b**) the intensity profile of the amplified seed pulse (bell-shaped green erratic curve) is depicted in comparison with the intensity profile of the initial pump (the blue curve), and (**c**) the power spectrum of amplified seed pulse for an initially ring shaped pump pulse.

Figure 2b shows the intensity profile of the output seed pulse in comparison with the intensity profile of the initial pump. One obtains a final seed intensity which is about five time larger than the initial pump intensity (see Fig. 2b). The comparison of the initial seed intensity (Fig. 2a) with the amplified seed intensity (Fig. 2b, green curve (color online)) shows that the intensity of the seed pulse has increased by six orders of magnitude from its initial value. The amplified pulse also shows a compression of initially picoseconds seed pulse due to interplay between group velocity mismatch and pump depletion. In the frequency domain, Figure 2c shows the output power spectrum of amplified short pulse.

Case 2: To explore the dependence of seed pulse amplification on the initial pump intensity, we have considered a higher order mode of pump pulse profile. We have performed a numerical simulation to study the amplification of a seed pulse counter-propagating to a long ring shaped pump. Recall that the pump field in the previous example had a Gaussian intensity distribution. When a short seed pulse interacted with a long Gaussian pulse, it appears planar near the region occupied by the seed. Therefore, most of the pump energy would not cause growth in the narrower seed pulse. For this simulation, considering the case of seed pulse amplification and compression through a counter-propagating ring shaped pump, we consider the longitudinal intensity distribution for pump field as:

$$A_0 A_0^* = A_{00}^2 \left(t^2/\tau_0^2\right) exp\left(-t^2/\tau_0^2\right),$$

where τ_0 is the pump width and A_{00} is the pump amplitude at $t = \pm \tau_0$. The minima of the initial ring shaped pump laser coincide with the peak of the seed laser. The seed pulse is initially considered to obey a Gaussian field distribution in this case while interacting with the counter propagating long ring pump. The results of this simulation are shown in Figure 3, which depicts the initial intensity profile of the seed pulse in time domain. Figure 3b shows the intensity profile of the output seed pulse in comparison with the intensity profile of the initial pump having a ring shaped intensity distribution. It is interesting to look at the result as shown in Figure 3b, where the seed pulse, is amplified across each maximum of pump. As Figure 3b shows a compression rate of 50 is obtained while a peak intensity of generated pulse is three times higher than initial pump peak intensity. The increase in intensity of amplified seed pulse is observed seven orders of magnitude higher than its initial value. Further amplification and compression is possible with pump laser of pulse length about 1–10 ps and intensity of pump about 10^{19} W/cm^2. However, 50-fold compression and three times amplification is also a promising result. Figure 3c shows the output power spectrum of amplified short pulse in the frequency domain.

4. CONCLUSIONS

We have presented a theoretical and numerical simulation of a Raman backscattering process in plasma as an amplification

https://doi.org/10.1017/S0263034609990292 Published online by Cambridge University Press

scheme for the ultraintense laser pulses. Our results indicate that the intensity profile of the pump laser is highly certain to achieve a high intensity, ultrashort pulse with a moderate total power in the pump. Numerical simulation shows a 50-fold pulse compression in the generated signal pulse with a peak power exceeding the pump laser. This simple model of pulse amplification has an advantage in practical applications to enable the construction of nearly table-top scale experiments with peak intensities above what is currently achieved with CPA amplifiers.

ACKNOWLEDGEMENT

This work was supported by a UK EPSRC Science and Innovation Award to the Centre for Plasma Physics, Queen's University Belfast (Grant No. EP/D06337X/1).

REFERENCES

Andreev, A.A. (2002). *Generation and Application of Ultrahigh Laser Fields*. New York: Nova Science.

Andreev, A.A., Bespalov, V.G., Ermolaeva, E.V. & Salomaa, R.R.E. (2007). Compression of ultraintense laser pulses in inhomogeneous plasma upon backward stimulated raman scattering. *Opt. Spectr*. **102**, 98–105.

Borisenko, N.G., Bugrov, A.E., Burdonskiy, I.N., Fasakhov, I.K., Gavrilov, V.V., Goltsov, A.Y., Gromov, A.I., Khalenkov, A.M., Kovalskii, N.G., Merkuliev, Y.A., Petryakov, V.M., Putilin, M.V., Yankovskii, G.M. & Zhuzhukalo, E.V. (2008). Physical processes in laser interaction with porous low-density materials. *Laser Part. Beams* **26**, 537–543.

Deutsch, C., Bret, A., Firpo, M.C., Gremillet, L., Lefebvre, E. & Lifschitz, A. (2008). Onset of coherent electromagnetic structures in the relativistic electron beam deuterium-tritium fuel interaction of fast ignition concern. *Laser Part. Beams* **26**, 157–165.

Eder, D.C., Amendt, P. & Wilks, S.C. (1992). Optical-field-ionized plasma x-ray lasers. *Phys. Rev. A* **45**, 6761–6772.

Eliezer, S., Murakaml, M. & Val, J.M.M. (2007). Equation of state and optimum compression in inertial fusion energy. *Laser Part. Beams* **25**, 585–592.

Faenov, A.Yu., Magunov, A.I., Pikuz, T.A., Skobelev, I.Yu., Gasilov, S.V., Stagira, S., Calegari, F., Nisoli, M., De Silvestri, S., Poletto, L., Villoresi, P. & Andreev, A.A. (2007). X-ray spectroscopy observation of fast ions generation in plasma produced by short low-contrast laser pulse irradiation of solid targets. *Laser Part. Beams* **25**, 267–275.

Giulietti, D., Galimberti, M., Giulietti, A., Gizzi, L.A., Labate, L. & Tomassini, P. (2005). The laser-matter interaction meets the high energy physics: Laser-plasma accelerators and bright X-gamma-ray sources. *Laser Part. Beams* **23**, 309–314.

Gorbunov, V.A., Papernyi, S.V., Petrov, V.F. & Startsev, V.R. (1983). Time compression of pulses in the course of stimulated Brillouin scattering in gases. *Kvantovaya Elektronika* **10**, 1386–1395.

Hora, H. (2007*a*). New aspects for fusion energy using inertial confinement. *Laser Part. Beams* **25**, 37–45.

Hora, H. (2007*b*). New aspects for fusion energy using inertial confinement. *Laser and Part. Beams* **25**, 327–328.

Joshi, C. (2006). Plasma accelerators. *Sci. Amer*. **294**, 41–48.

Kalashnikov, M., Osvay, K. & Sandner, W. (2007). High-power Ti:Sapphire lasers: Temporal contrast and spectral narrowing. *Laser Part. Beams* **25**, 219–223.

Key, M.H., Cable, M.D., Cowan, T.E., Estabrook, K.G., Hammel, B.A., Hatchett, S.P., Henry, E.A., Hinkel, D.E., Kilkenny, J.D., Koch, J.A., Kruer, W.L., Langdon, A.B., Lasinski, B.F., Lee, R.W., Macgowan, B.J., Mackinnon, A., Moody, J.D., Moran, M.J., Offenberger, A.A., Pennington, D.M., Perry, M.D., Phillips, T.J., Sangster, T.C., Singh, M.S., Stoyer, M.A., Tabak, M., Tietbohl, G.L., Tsukamoto, M., Wharton, K. & Wilks, S.C. (1998). Hot electron production and heating by hot electrons in fast ignitor research. *Phys. Plasmas* **5**, 1966.

Kline, J.L., Montgomery, D.S., Rousseaux, C., Baton, S.D., Tassin, V., Hardin, R.A., Flippo, K.A., Johnson, R.P., Shimada, T., Yin, L., Albright, B.J., Rose, H.A. & Amiranoff, F. (2009). Investigation of stimulated Raman scattering using a short-pulse diffraction limited laser beam near the instability threshold. *Laser Part. Beams* **27**, 185–190.

Maier, M., Kaiser, W. & Giordmaine, J.A. (1966). Intense light bursts in the stimulated Raman effect. *Phys. Rev. Lett*. **17**, 1275–1277.

Mourou, G.A., Barty, C.P.J. & Perry, M.D. (1998). Ultrahigh-intensity lasers: Physics of the extreme on the tabletop. *Phys. Today* **51**, 22–28.

Ren, J., Cheng, W., Li, S. & Suckewer, S. (2007). A new method for generating ultraintense and ultrashort laser pulses. *Nat. Phys*. **3**, 732–736.

Renner, O., Juha, L., Krasa, J., Krousky, E., Pfeifer, M., Velyhan, A., Granja, C., Jakubek, J., Linhart, V., Slavicek, T., Vykydal, Z., Pospisil, S., Kravarik, J., Ullschmied, J., Andreev, A.A., Kampfer, T., Uschmann, I. & Forster, E. (2008). Low-energy nuclear transitions in subrelativistic laser-generated plasmas. *Laser Part. Beams* **26**, 249–257.

Rodriguez, R., Florido, R., Gll, J.M., Rubiano, J.G., Martel, P. & Minguez, E. (2008). RAPCAL code: A flexible package to compute radiative properties for practically thin and thick low and high-Z plasmas in a wide range of density and temperature. *Laser Part. Beams* **26**, 433–448.

Romagnani, L., Borghesi, M., Cecchetti, C.A., Kar, S., Antici, P., Audebert, P., Bandhoupadjay, S., Ceccherini, F., Cowan, T., Fuchs, J., Galimberti, M., Gizzi, L.A., Grismayer, T., Heathcote, R., Jung, R., Liseykina, T.V., Macchi, A., Mora, P., Neely, D., Notley, M., Osterholtz, J., Pipahl, C.A., Pretzler, G., Schiavi, A., Schurtz, G., Toncian, T., Wilson, P.A. & Will, O. (2008). Proton probing measurement of electric and magnetic fields generated by ns and ps laser-matter interactions. *Laser Part. Beams* **26**, 241–248.

Ross, I.N., Matousek, P., Towrie, M., Langley, A.J. & Collier, J.L. (1997). The prospects for ultrashort pulse duration and ultrahigh intensity using optical parametric chirped pulse amplifiers. *Opt. Commun*. **144**, 125–133.

Seifter, A., Kyrala, G.A., Goldman, S.R., Hoffman, N.M., Kline, J.L. & Batha, S.H. (2009). Demonstration of symcaps to measure implosion symmetry in the foot of the NIF scale 0.7 hohlraums. *Laser Part. Beams* **27**, 123–127.

Shvets, G., Fisch, N.J., Pukhov, A. & Mayer-Ter-Vehn, J. (1998). Superradiant amplification of an ultrashort laser pulse in a plasma by a counterpropagating pump. *Phys. Rev. Lett*. **81**, 4879–4882.

Strickland, D. & Mourou, G. (1985). Compression of amplified chirped optical pulses. *Opt. Commun*. **56**, 219–221.

Tajima, T. (1985). High energy laser plasma accelerators. *Laser Part. Beams* **3**, 351–413.

Winterberg, F. (2008). Lasers for inertial confinement fusion driven by high explosives. *Laser Part. Beams* **26**, 127–135.

Zvorykin, V.D., Didenko, N.V., Ionin, A.A., Kholin, I.V., Konyashchenko, A.V., Krokhin, O.N., Levchenko, A.O., Mavritskii, A.O., Mesyats, G.A., Molchanov, A.G., Rogulev, M.A., Seleznev, L.V., Sinitsyn, D.V., Tenyakov, S.Y., Ustinovskii, N.N. & Zayarnyi, D.A. (2007). GARPUN-MTW: A hybrid Ti:Sapphire/KrF laser facility for simultaneous amplification of subpicosecond/nanosecond pulses relevant to fast-ignition ICF concept. *Laser Part. Beams* **25**, 435–451.

https://doi.org/10.1017/S0263034609990292 Published online by Cambridge University Press